

Preparation of activated carbons for storage of methane and its study by adsorption calorimetry

Juan Carlos Moreno-Piraján¹ · Marlon José Bastidas-Barranco² · Liliana Giraldo³

Received: 27 September 2016 / Accepted: 29 January 2017 / Published online: 13 February 2017
© Akadémiai Kiadó, Budapest, Hungary 2017

Abstract The scope of this investigation is to relate textural and surface characteristics of activated carbon prepared from Cerrejon coal (Colombia) to their methane quantity adsorption. Sub-bituminous coal from the Cerrejon coal mine in Colombia was used as a raw material for the preparation of pore size-controlled activated carbon adsorbents. A subsequent chemical treatment was carried out, after making a physical activation with CO₂. Samples were treated with CO₂ flow at 850 °C by varying activation time to achieve different burn-off activated carbons. The samples chemically activated with H₃PO₄ under CO₂ atmosphere showed higher activation rates, surface area, and micropore volume compared to other activation methods, although not all the samples prepared by this method presented storage quantities methane in function of surface area development. Moreover, it was shown that using small proportion of KCl and H₃PO₄ creates an initial narrow microporosity. Further physical activation grants better development of pore structure. In terms of pore size distribution, the combined preparation method resulted in a better and more homogenous pore size distribution than the conventional physical activation method. Controlling the pore size of activated carbon by this combined activation technique can be utilized for tuning the pore size

distribution. Storage studies of methane up to 60 bar were realized. It was concluded that the high surface area and micropore volume of activated carbons do not unequivocally determine methane capacities. Adsorption microcalorimetry is a useful technique to follow the process of the adsorption reaction of CH₄, and its results are in agreement with the results found study by adsorption at high pressure.

Keywords Adsorption calorimetry · Storage methane · Isotherms · Coal

Introduction

Colombia is the fourth largest coal exporter, and therefore, part of its energy capacity is based on this material. In the densely populated urban areas, the natural gas is usually available for domestic purposes [1, 2]. However, in the rural areas, coal and the liquefied petroleum gas (LPG) have become one of the major fuels for domestic cooking and heating because there are no gas pipelines available and it cannot be justified to develop it in terms of its capital investment and returned benefit. Therefore, an efficient storage vessel is an alternative way to provide natural gas in the rural areas [1, 3]. There are four options available for selection in storing natural gases—liquefied natural gas (LNG), compressed natural gas (CNG), gas to solids (GtS) and adsorbed natural gas (ANG). In consideration of safety in the home environment, the LNG, which requires a low temperature, and the CNG, which requires a high pressure, can be excluded from the list. The adsorbed natural gas (ANG) shows its potential as a way for storing natural gas because of its higher energy density under a much lower pressure than CNG [1, 4]. There are many papers on the

✉ Juan Carlos Moreno-Piraján
jumoreno@uniandes.edu.co

¹ Facultad de Ciencias, Departamento de Química, Grupo de Investigación en Sólidos Porosos y Calorimetría, Universidad de los Andes (Colombia), Bogotá, CO, USA

² Facultad de Ingeniería, Grupo DESTACAR, Universidad de La Guajira (Colombia), La Guajira, CO, USA

³ Facultad de Ciencias, Departamento de Química, Universidad Nacional de Colombia (Colombia), Bogotá, CO, USA

application of ANG technique to motor vehicles. The research mainly focuses on searching for high-performance adsorbents by way of management of thermal effect from adsorption and desorption. Adsorbents used are the highly microporous activated carbons with relatively high packing densities and specific surface area [1, 5–9]. Since the process of adsorption and desorption accompanies with transfer of heat, the temperature of the adsorbent bed fluctuates. It decreases the useable capacity of the storage system accordingly. Therefore, the minimization of thermal effect is considered as a key in developing an ANG storage system for commercial purpose [1, 10–13]. Various materials are used to fulfill this type of requirements. The activated carbons obtained from carbon mineral are interesting materials from this point of view, because the track of activation generates activated carbons with properties that can be controlled so as to analyze their applicability in the storage of energy. The physical activation is a widely used method for the preparation of activated carbons (AC).

Physical activation of AC consists of two steps: The first step is the elimination of most of the hydrogen and oxygen contents by pyrolysis of carbonaceous material at high temperature and inert atmosphere. The second step is to activate the chars at high temperature and in the presence of steam or carbon dioxide as oxidizing gasses. Carbon atoms are extracted by these agents from the structure of the porous carbon according to the following endothermic reactions [14–16]:



This method of activation, entirely within the gas phase, is known as thermal or physical activation [15, 16]. Chemical activation involves the treatments of precursor with a chemical agent followed by conventional heat treatment which will affect the process of carbonization and generates the porosity [17–19]. Among the numerous dehydrating agents, phosphoric acid and chlorides metallics (of zinc, calcium and potassium, etc.) are widely used for the production of ACs, especially for lignocellulosic and cellulosic precursors [17, 20–22]. On the other hand, combination of chemical and physical activation is another technique to prepare highly microporous AC. In line with the observations in this field, there are scarce studies that use combination of these two methods [1, 17, 21], and as far as author knowledge, there is no information concerning the effects of using this method with coal mineral-type sub-bituminous as raw material and methane adsorption capacity. So far, in the works reported in the literature, chemically activated carbons from oil palm shell as a precursor have been prepared using low concentration of

zinc chloride or phosphoric acid as activating agent [21, 23]. The prepared samples were heated under CO_2 for physical activation at different durations, and adsorption studies of methane was carried out at low pressure to characterize the samples. Gas adsorption at low pressure was chosen because it can depict the effect of pore size distribution on methane adsorption capacity (at low pressure, the smallest pores will be filled first).

In the present study, the appropriate chemical ratio and preparation conditions have been tuned to prepare microporous activated carbons (ACs) with high surface area, narrow micropore size distribution (MPSD) and good methane adsorption capacity. Conventional physical activated coal from Cerrejon mine (Colombia) is compared to chemically activated Cerrejon mine (Colombia) combined with physical activation. This aimed at improving the microporosity of the produced AC to increase the methane adsorption. In this research, further adsorption microcalorimetry is used as an alternative technique to explore whether it is possible to follow the processes of methane storage on samples prepared in this work.

Experimental

Materials

Coal was supplied by the “Cerrejon coal mine” in Colombia and was used as a raw material. Were crushed and sieved to a particle size in the range of 1–4 mm, then washed carefully and dried at 110 °C for 48 and phosphoric acid (H_3PO_4) 85% by mass solution in water supplied by Merck Millipore were used for chemical activation.

Experimental setup

Two different 310 stainless steel reactors were used in this work to have better heat treatment; the first one with 6.3 cm i.d. was used for the chemical activation and carbonization process (precursor amount more than 150 g). For CO_2 activation, a second reactor with 2.5 cm i.d. was used. Both reactors have gas distributor located in the center. These distributors are covered with fine mesh stainless steel wire. The K-type thermocouple controls the temperature inside the reactor. The reactor is designed for batch operation and centrally positioned within an enclosing vertical tube electrical furnace (Carbolite VST 12/900). The system can be operated to a maximum temperature of 1200 °C. For preheating of CO_2 during physical activation, the stainless steel pipeline passes through an oven (Heraeus D-6450) to heating up to 850 °C and feed to the reactor.

Preparation of activated carbons (ACs) from coal (Cerrejón, Colombia)

Chemical activation

For chemical activation, the coal (Cerrejón, Colombia) was first impregnated with a standard solution of chemicals (2 mL per gram of the precursor). The chemicals per gram of coal mass ratios are indicated as XK and XP for the potassium and phosphorous, respectively. A mixture of precursor and chemical solution of $XK = 0.25$ or $XP = 0.09$ [21, 24] was stirred for 6 h at 80 °C, and then, temperature was increased to the boiling point until complete dryness. In the next step, the impregnated materials with KCl and H_3PO_4 were heated up to 550 °C and 500 °C, respectively, for 4 h (heating rate of 5 °C min^{-1}) under N_2 flow rate of 100 mL min^{-1} [15, 18, 21]. The chemically prepared ACs were washed several times with abundant amount of distilled water to remove the excess activating agent and increase the pH over 6. For the KCl samples, to increase the solubility of K, activated carbons were first washed with 0.1 N solution of HCl followed by distilled water washing until the absence of chloride ions in the washing water as indicated by its pH [16, 20, 24].

Physical activation

The prepared coal (Cerrejón, Colombia) and the products of chemical activation were first carbonized at 950 °C for 1 h and heating rate of 10 °C min^{-1} [14, 15]. After carbonization, the resulting products were taken out and used for thermal activation under carbon dioxide stream. For physical activation, 60 g samples were heated up to 850 °C, and then, carbon dioxide stream with flow rate of 100 mL min^{-1} was used for 3–12 h (heating rate of 10 °C min^{-1}) to obtain activated carbons with different burn-offs.

In order to facilitate the description of the prepared activated carbons, it is necessary to use abbreviations in nomenclature of these activated carbons. ACK and ACP denote the series of activated carbon from coal (Cerrejón Colombia)-based activated carbons obtained by potassium chloride and phosphoric acid activation followed by carbon dioxide activation, respectively. AC denotes the activated carbon obtained by physical activation of coal. Activation time (expressed in hours) is written as a suffix for the two letters (example: ACK-12 represents potassium chloride activated sample with further activation under carbon dioxide for 12 h).

Characterization of activated carbons

The development of porosity on the activated carbons was evaluated by nitrogen adsorption measurements at

–196 °C using a sortometer IQ2 (Quantachrome, Boynton Beach, FL, USA). The samples were previously degassed for 6 h at 300 °C. Nitrogen adsorption data were used to determine: (1) the total pore volume (V_t) at a relative pressure of 0.95, (2) the BET specific surface area (S_{BET}), according to the criteria established by Rouquerol et al. [10], and (3) the micropore volume ($V_{N_2,DR}$), pores <2 nm, by the application of the Dubinin–Radushkevich equation (DR) [11]. The difference between V_t and $V_{N_2,DR}$ is considered to be the mesopore volume (V_{meso}). The volume of narrow micropores, pores <0.7 nm, was calculated by applying DR equation to the CO_2 adsorption data at 0 °C ($V_{CO_2,DR}$). The characteristics curves of N_2 and CO_2 isotherms (LnV vs $A2/\beta2$) for representative samples were evaluated. Pore size distribution was calculated by the application of the quenched solid density functional theory (slit pore, QSDFT equilibrium model) to the nitrogen adsorption isotherm data [9, 10] for pores >1 nm and the nonlinear density functional theory (NLDFT) to the CO_2 adsorption isotherm data for pores <1 nm.

Methodological description of adsorption isotherms of CH_4

The methane quantity adsorbed of the synthesized activated carbons was estimated from the methane adsorption isotherms at 25 °C and up to a pressure of 1 and/or 60 Bar. Before any adsorption measurement, activated carbons were degassed at 300 °C for 6 h in a volumetric system HPVA 100, from VTI, after outgassing for 6 h at 300 °C and a final pressure of 10^{-8} Pa. The delivery of methane was calculated by subtracting the volume remaining after desorption at atmospheric pressure from the quantity adsorbed at 1 and/or 60 Bar.

Measurement of differential enthalpies of adsorption with methane

A Tian–Calvet heat-flow microcalorimeter is an example of a high-sensitivity apparatus, which is suitably adapted to the study of gas–solid interactions. In this work, an adsorption microcalorimeter is used that is “homemade.” The instrument described is not only far less expensive than commercial systems, but also has some features that are not found in those systems. This calorimeter was connected to a sensitive volumetric commercial system: a sortometer IQ2 (Boynton Beach, Miami, USA) [23–26]. Volumetric and calorimetric data were measured simultaneously using the “homemade” adsorption microcalorimeter, connected to a IQ2 sortometer (residual pressure $p \leq 10^{-6}$ Torr) (see Fig. 1) [15, 16, 24, 25]. During the same experiment, both differential heat adsorption evolved and adsorption isotherm are measured simultaneously from the gas or vapor phase that is applied to the system. Microcalorimetry

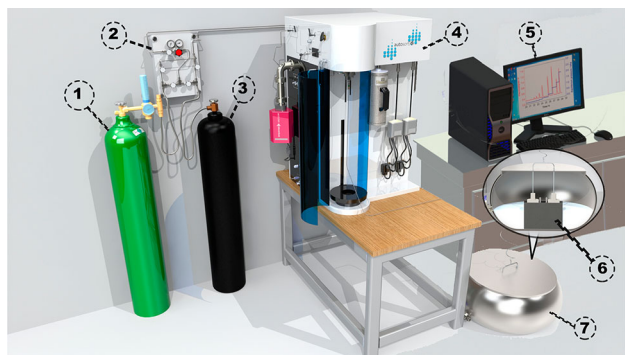


Fig. 1 Adsorption microcalorimetry setup used to determine the heat differential between methane and the prepared samples

employs two identical calorimetric cells: one containing the sample under investigation, i.e., ACK, ACP or AC to be tested, and the other (usually empty, through which the gas or vapor is passed) serving as reference cell, was connected in opposition [20, 26]. These cells are constructed in quartz to avoid physical or chemical interactions. As it is a differential calorimeter Tian–Calvet type, all parasitic phenomena (i.e., all thermal effects other than the one due to the interaction of the gas with the solid surface) were successfully compensated. This “homemade” microcalorimeter allows measurements of adsorption heat in a range from room temperature to 500 °C. The adsorptive pressure in the measurements was monitored by the sortometer IQ2 (Quantachrome, Boynton Beach, USA).

Before each experiment, the samples were outgassed with a heating rate of 1 °C min⁻¹ and the temperature was ramped up from 0 °C to 250 °C. Once 250 °C was reached, it was kept at this temperature for 12 h. Afterward, it was cooled down to room temperature at the same rate. The experiments were carried out isothermally by admitting stepwise increasing doses of the adsorbate gas to the sample previously evacuated. The initial dose sent to the system was 20 mbar. Since the initial doses were small enough, the heat obtained could be considered as a differential enthalpy of adsorption. At each dose, the equilibrium pressure was added to the sending incremental dose (20 mbar). Afterward, the dose amount was increased to 360 mbar and the procedure was repeated until no further pressure drop was observed. The heat evolved by each dose was measured, and the corresponding amount adsorbed was obtained by the pressure drop in the known volume of the equipment. For each dose, thermal equilibrium was attained before the pressure p_i (initial pressure); the adsorbed amount δn_{ads} and the integral heat evolved δQ_{int} were measured. The adsorption experiments were concluded when a relatively high pressure was reached without a significant evolution of heat, and the adsorbed amount became negligible [15, 16, 19, 20, 24, 25, 27, 28].

In order to determine the differential enthalpies of adsorption from the data obtained by microcalorimetry, the measured enthalpy was divided by the quantity of adsorbed molecules of methane for each dose. The heat was determined by integrating the calorimetric data, and the quantity of adsorbed molecules was calculated using the collected pressure data. Amounts adsorbed were expressed as mmol.g⁻¹ by samples outgassed at 300 °C.

The calorimetric data were reported here as differential heats, $q_{\text{diff}} = \delta Q_{\text{int}}/\delta n_{\text{ads}}$. Hence, the differential enthalpy of adsorption is defined as the enthalpy change going from the gas phase to the adsorbed phase. They can also be reported as integral heats of adsorption, Q_{int} . A stepwise procedure was followed in this study [15, 25].

In Fig. 1, the components of the microcalorimetry system are shown; they are the pressure control panel, electric system, microcalorimetry and IEEE device required for transferring data.

Result and discussion

Effect of activation method on activation rate

The graph of activation time and burn-off for three different methods of KCl and H₃PO₄ activation continued by CO₂ activation and physical activation of coal (Cerrejón, Colombia) was realized. All of these methods represent almost linear correlation between activation time and burn-off. The slope of each curve illustrates the activation rate [15, 16, 20, 24–26, 29]. The total mechanism of physical activation depends on how the gasification agent (gas) molecule gains access to an internal carbon atom and the facility at that site for reaction to take place leading to the removal of a carbon atom. Therefore, it can be said that a matter of fundamental importance concerns the state of carbon surface during the course of a gasification reaction. It has been shown that in normal pressure (not vacuum condition), carbon dioxide reaction with carbon molecules would be influenced or controlled by mass and energy transfer. Since all the samples were prepared in the same temperature and atmospheric conditions, the difference in the rate of gasification need to be explained. The difference in surface structures can be one of the reasons that cause difference in reactivity (expressed as rate of gasification per square meter of surface) during the course of the reaction. Although chemically activated samples were washed carefully after the chemical activation process, some inorganic compounds such as phosphorous and potassium remain inside the carbon. These impurities may act as catalysts for the oxidation and consequently reduce number of active sites [15, 16, 20, 24–26, 29]. These chemicals traces may have some effect on the rate of

thermal activation. In the case of potassium chloride activated samples, the remaining activated agents may have unenthusiastic effects that cause limitation in access of CO_2 to the reactive sites and consequently reduction in rate of gasification. In the case of chemical activation using phosphoric acid, as the temperature of the sample increases, the excess phosphoric acid is converted to pyrophosphoric acid ($\text{H}_4\text{P}_2\text{O}_7$) by condensation and dehydration. Extended heating forms polyphosphoric acid ($\text{H}_n + 2\text{P}_n\text{O}_{3n+1}$), which finally decomposes to form P_2O_5 that sublimates above $300\text{ }^\circ\text{C}$ and melts and vaporizes at $580\text{--}585\text{ }^\circ\text{C}$ [21, 25, 30]. Since the chemical activation temperature is $450\text{ }^\circ\text{C}$, some of these materials remain after activation. In carbonization process, although the temperature increases to $900\text{ }^\circ\text{C}$, there is no flowing gas to remove them out of the carbonized samples. It was noticed that a white color flame formed at the exhaust pipe during physical activation. This flame can be due to the effect of flowing CO_2 gas during activation which extracts P_4 (g). This extraction of the remained chemicals during physical activation may cause higher mass loss in these samples and affect the rate of physical activation. In addition, KCl activated samples show higher total mass loss in chemical activation and carbonization process (79% burn-off) in comparison with coal char samples in the carbonization process (70% burn-off). Subsequently, it can be inferred that higher percentage of tar contents are degraded in the chemically activated sample which causes higher surface area and more reaction sites compared to the palm shell char. The surface area of potassium chloride and phosphoric acid activated sample after carbonization process was $645\text{ m}^2\text{ g}^{-1}$ and $1174\text{ m}^2\text{ g}^{-1}$, respectively. Because of that during pyrolysis occurs the breaking of C–C bonds, as well as weaker carbon–oxygen bonds and carbon–carbon (aliphatic), the breaking of the carbon–oxygen bonds is the most important in type “Cerrejon mine” coals. Consequently, pyrolysis products of these coals are characterized by high water content, low tar content, low molecular weight aromaticity index and a highly porous isotropic solid structure. Therefore, it can be concluded that thermal activation of H_3PO_4 activated samples showed higher rate of activation compared to the two other types of activation of KCl.

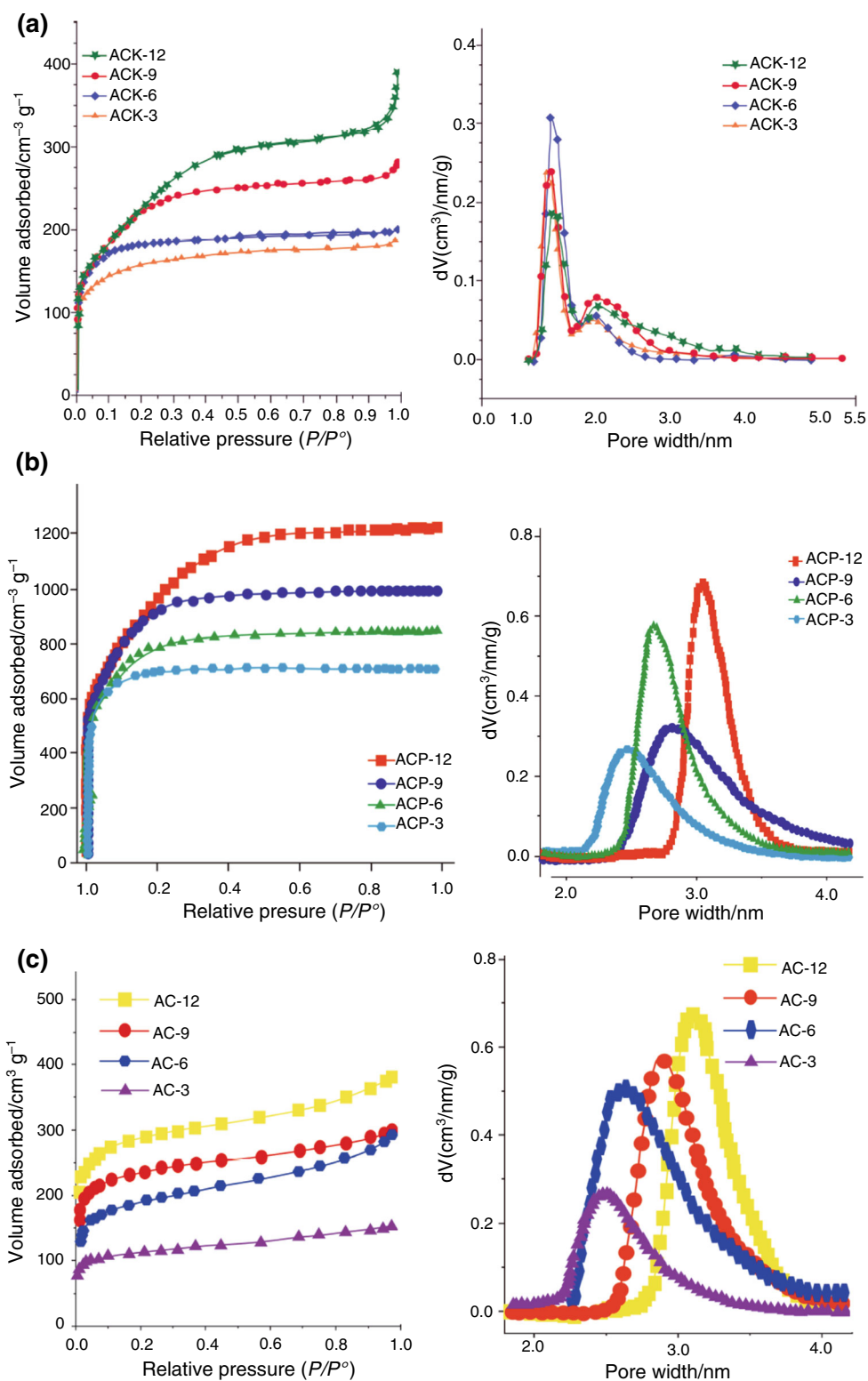
Nitrogen adsorption isotherms

Figure 2a shows the nitrogen adsorption isotherms of ACK samples. Similar to typical activated carbons, ACK samples exhibit almost horizontal plateau at higher relative pressures, showing type Ib isotherm according to the IUPAC classification that indicates highly microporous materials with a narrow pore size distribution [31]. The isotherms have the following behavior: The quantity

capacity increases with increasing activation time at each relative pressure which indicates the widening of microporosity. It is observed that ACK series have similar behavior; it can be to infer that all of these samples include micropores. The results show that there is a slight difference between the samples ACK-6 and ACK-3 and both low and high relative pressures, which shows microporosity either common in narrow or large micropores. The isotherms of Fig. 2a show that as the activation time is increased, nitrogen adsorption micropore volume increases as well. It suggests that the number of micropores increases with the activation time. Comparing the isotherms of samples ACK-9 and ACK-12, you can see that it presents an increased N_2 adsorbed at higher relative pressures in the ACK-12 sample. This reflects a widening in the micropores because of the activation time. The ACP series activated carbons (shown in Fig. 2b) have a similar behavior to that of the analyzed series, ACK, at low burn-off degree. The samples ACP-3 and ACP-6 are type Ib adsorption isotherm, showing the difference in the quantity capacity at low relative pressure. ACP-6 attained higher quantity capacity as compared to ACP-3, at relative pressures >0.25 . This indicates that the increase in burn-off causes widening of micropores. This increase in nitrogen quantity capacity is continued up to ACP-12. Analyzing the isotherms of samples ACP-6 and ACP-9 they have very similar at very low relative pressures and then above relative pressure $P/P^\circ = 0.4$ isotherms become parallel. This behavior means that the differences are in the large size micropores [24]. Moreover, it is interesting to analyze the behavior of the ACP-12 sample, which shows a constant and gradual increase in nitrogen which makes this isotherm corresponds more to a type Ib (at low pressures) combined with a type II (at high pressures) according to the last recommendations of the IUPAC. The change in the shape of the isotherm of this sample is probably due to the treatment to prepare it, during which the textural characteristics were modified.

Figure 2c shows the nitrogen isotherms of the AC series of the samples prepared in this work. The increase in nitrogen adsorption is significant at all pressure range. Therefore, the isotherms for AC-3, AC-6, AC-9 and AC-12 are characterized by type Ib isotherms (for AC-3) and by type Ib (at low pressures) combined with type II isotherms (at high pressures) for the AC-6, AC-9 and AC-12 samples. In summary, the difference between the first three samples (AC-3, AC-6 and AC-9) is only clear at low pressure ($P/P^\circ < 0.3$). At higher relative pressures, they become parallel (linear region), as was analyzed before in some of the samples prepared. For AC-12 sample, the difference in nitrogen quantity adsorption with other samples either at low or high pressure (knee of isotherm and slope of linear portion, respectively) is considerable, which indicates the

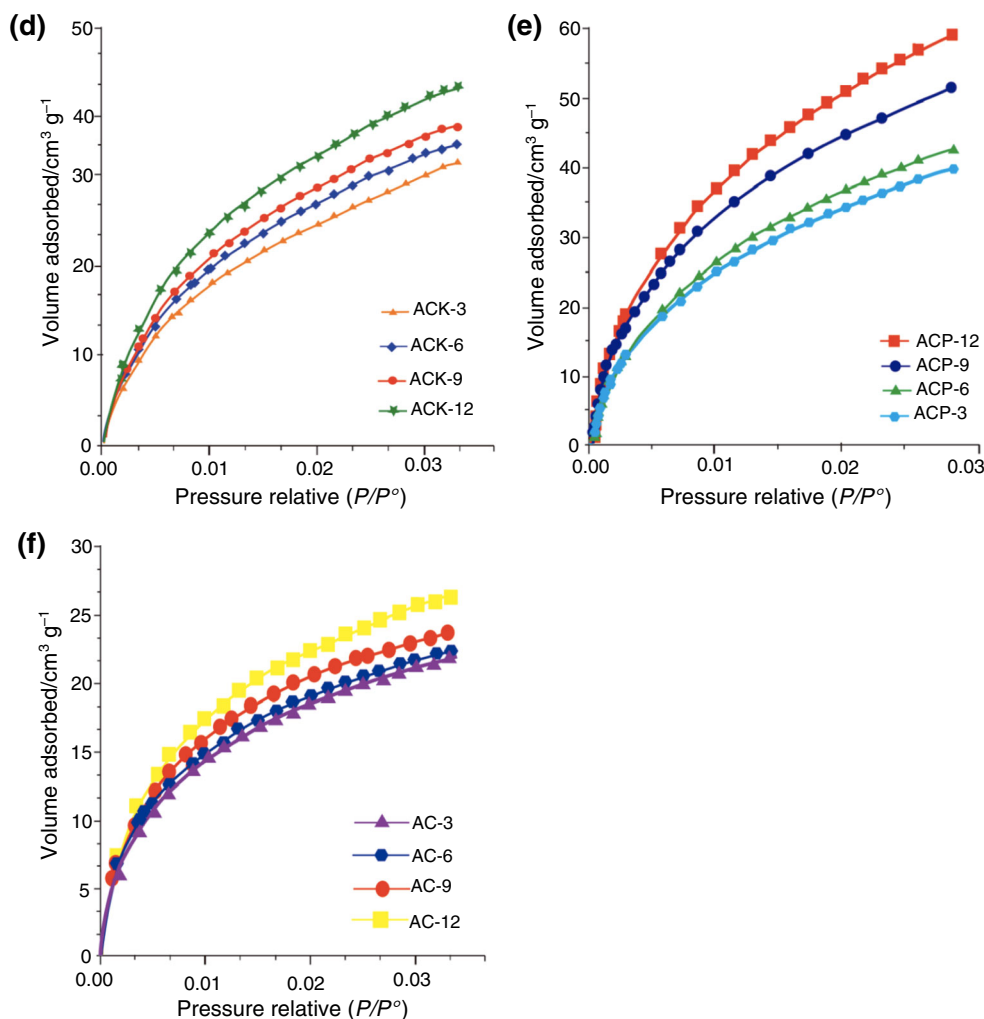
Fig. 2 **a** N_2 adsorption isotherms of KCl activated carbons followed by CO_2 activation at different times. **b** N_2 adsorption isotherms of H_3PO_4 activated carbons followed by CO_2 activation at different times. **c** N_2 adsorption isotherms of CO_2 activated carbons at different times. Also, pore size distribution of ACK, ACP and activated carbons, respectively. **d** CO_2 adsorption isotherms of KCl activated carbons followed by CO_2 activation at different times. **e** CO_2 adsorption isotherms of H_3PO_4 activated carbons followed by CO_2 activation at different times. **f** CO_2 adsorption isotherms of CO_2 activated carbons at different times



outstanding growth of narrow and larger micropores as compared with other samples. Although nitrogen adsorption for AC-12 is the highest among the rest of the AC series, there is still large difference with ACP series nitrogen capacity. Each carbon from series ACP has a

larger quantity adsorption than the equivalent activation time of the two other series (ACK and AC series), although the differences are smaller in the case of AC carbons. As far as nitrogen quantity adsorption at approximate similar burn-off degree of these three samples is concerned, ACP

Fig. 2 continued



ACs exhibit the best adsorption results. For example, ACP-6 and AC-9 have close burn-off degree; however, quantity adsorption of ACP-6 is much higher.

The isotherms at low pressures (up to $P/P^o = 0.03$) are shown in Fig. 2c–f, shows a pressure range where information about the ultramicroporosity (pores smaller than 0.7 nm) can be obtained. Samples corresponding to ACP-9, ACK-9 and ACK-12 (see Table 1) present the largest narrow micropore volume (V_n) and therefore show the highest CO₂ adsorption. Other adsorbents with a higher ultramicroporosity, like AC-6 sample, do not adsorb the same amount of CO₂ due to its minor surface area value. Therefore, it can be said that the adsorption of CO₂ is function not only a high narrow micropore volume but also surface area.

Textural characterization

Table 1 shows the textural parameters: the surface area, micropore and pore volume of activated carbons prepared from coal of Cerrejon mines (Colombia) samples.

Although the ACK samples possess expected surface area values within the normal range, all of the preparation methods show high relative micropores. On the other hand, ACK-9 and ACK-12 show higher value of micropore volume and surface area compared to other conditions in this series. The ACK series shows only a slight variation in the micropore volume developed on the increase in activation time, which shows that this variable regarding the activating agent does not have a strong effect on the development of micropore volume. As the time of activation increases from ACK-3 to ACK-6, it only presents a small difference between its micropore volume values. However, there is an increase in BET surface area amount and micropore volume values from ACK-6 to ACK-12. It can also be noticed that all products exhibit low mesopore volume. This could be due to the use of carbon dioxide as activating agent. Larger mesopore volume could be generated if steam is used as the activating agent [15, 20, 21]. In the ACP series, total volumes they develop (above 0.70 cm³ g⁻¹), are much higher than reported in the literature for similarly obtained materials. ACP-6 and ACP-9

Table 1 Preparation, production burn-off, surface area, pore volume of activated carbon

Sample	Burn-off/%	Nitrogen adsorption data at 77 K			CO ₂ adsorption data at 273 K	
		S _{BET} /m ² g ⁻¹	V _{Micro} /cm ³ g ⁻¹	V _{Total} /cm ³ g ⁻¹	Width/nm	V _n /cm ³ g ⁻¹
ACK-3	1.2	645	0.38	0.40	1.10	0.34
ACK-6	8.5	685	0.40	0.41	1.23	0.37
ACK-9	13.4	785	0.43	0.45	1.34	0.40
ACK-12	14.5	1084	0.46	0.42	1.45	0.44
ACP-3	22.4	1176	0.64	0.66	2.52	0.57
ACP-6	35.3	1387	0.79	0.83	2.75	0.78
ACP-9	57.8	1437	0.83	0.85	2.84	0.75
ACP-12	65.1	1174	0.59	0.64	3.21	0.56
AC-3	8.3	589	0.29	0.32	2.55	0.24
AC-6	26.5	658	0.34	0.35	2.67	0.29
AC-9	36.2	833	0.41	0.43	2.88	0.36
AC-12	43.2	1245	0.49	0.51	3.15	0.42

samples have values as high as 0.79 and 0.83 cm³ g⁻¹, respectively. In ACP series, due to the creation of new micropores and widening of narrow micropores, increase in both surface area and micropore volume from ACP-3 to ACP-6 is very high. Although there is an increase in micropore volume in ACP-9 compared to ACP-6, this increase is less than in the two former samples. ACP-9 has a higher mesopore and total pore volume than ACP-6, which is because increasing burn-off higher than 35.3% creates some new pores being mesoporous and widens some micropores to form mesopores. This is in good accordance with results already reported in the literature. The rate of mesopore development is higher for ACP-9 to ACP-12, and the BET surface area is lower with a microporosity of 88% ($V_{\text{Micro}}/V_{\text{Total}}$). It is clear that ACP-6 is a highly microporous material with a microporosity value of 97%, while ACP-12 has a lower microporosity of 88% and consequently more mesopore volume as shown in Table 1. ACP-9 possesses the highest surface area, pore volume and micropore volume among all ACP series. It also attained better microporous ACs compared to previously published biomass raw material-based AC. Finally, in the AC series can be seen that both the volume of micropores as superficie area constantly changing from AC-3 to AC-12. After 12 h of coal (Cerrejon) char activation under carbon dioxide, micropore volume and surface area values are lower than that activated by phosphoric acid samples. As previously mentioned, nitrogen adsorption isotherms of the AC series exhibited continuous increase in surface area, pore volume and micropore volume when the burn-off increased up to 43.20%. The elimination almost every volatile during the carbonization step at 900 °C and the increase in the surface area should be related to the CO₂ gasification process. Table 1 shows that the burn-off

percentage, micropore volume, surface area and pore volume increase by increasing activation time, but this increase is higher from AC-9 to AC-12. Increasing the activation time to 12 h causes the deeper CO₂ gasification and improvement in creation of further new pores. As a result, there would be acceleration in the development of the AC porosity. The pore size distribution is defined as structural heterogeneity of the porous material and closely related to both equilibrium properties and kinetics of these materials used in industrial applications. Figure 3 presents the pore size distribution of ACK-6, ACP-9 and AC-12 samples which achieved the highest micropore volume in each type of sub-bituminous coal activation. All of the pore size distribution curves of AC have their maximum at the pore diameter between 1 and 3 nm, indicating the presence of micropores. From this figure, it is apparent that the activation method had significant effect on the pore structure of the produced ACs. Figure 2 also shows that the pore size distribution in the chemically activated samples ACK and ACP is more homogenous compared to the physical AC. In ACK and ACP samples, using small amount of potassium chloride or phosphoric acid for chemical activation generated basic pore structure. This structure develops more by the physical activation that follows [34]. On the other hand, between ACK-9 and ACP-9, the first is more homogenous because of lower activation degree and lack of mesopores. Higher degree of burn-off in ACP-12 compared with the two other samples caused the creation of micropore structure and widening of micropores to mesopores, and consequently, the total pore volume increased [28].

The width of pore diameter of samples in each type of activation increases by increasing the activation time as shown in Table 1. ACs derived from coal from Cerrejon

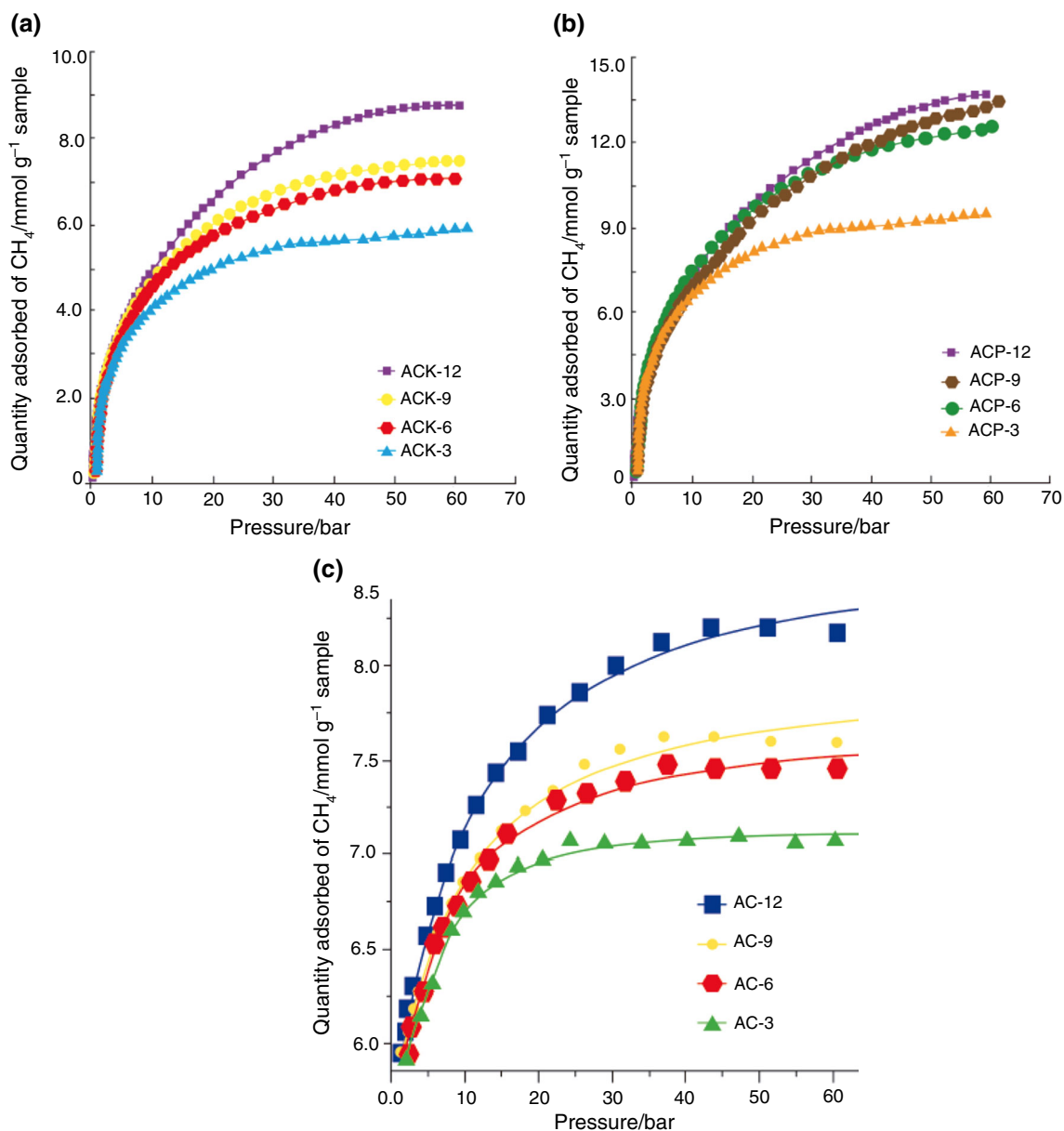


Fig. 3 **a** Methane adsorption isotherms of ACK series of activated carbons at different pressures. **b** Methane adsorption isotherms of ACP series of activated carbons at different pressures. **c** Methane adsorption isotherms of AC series of activated carbons at different pressures

(Colombia) and activated by H_3PO_4 followed by physical activation showed larger mean pore diameter (2.52–3.21 nm) in comparison with those activated first by KCl and then by CO_2 (1.10–1.45 nm) and just CO_2 activated coal (Cerrejón) chars (2.55–3.15 nm).

On the other hand, the PSD was calculated using the QSDFT (quenched solid density functional theory) and non-local density functional theory (NLDFT) kernels for each of the samples prepared in this work (not included here). The best fit results were the distributions with the QSDFT. The results calculated with the NLDFT and QSDFT kernels showed that the mean pore width differs very little, although its magnitude is found within

microporous materials, specifically within ultramicropores. These results are consistent with the shape of the N_2 adsorption isotherms obtained at 77 K for the samples of this investigation, which as mentioned above correspond to essentially microporous materials. Calculations were made with these algorithms for the volumes assuming cylindrical, slit and cylindrical-slit pores using the NLDFT and QSDFT models, better fitting the cylindrical pore.

Methane adsorption

Methane is an organic molecule of nonpolar character that during adsorption (physisorption or chemisorption) may be

deposited on the surface of an activated carbon. The results taken with HPVA in our research allow to establish the quantity adsorption on each of the prepared samples. To perform this study in detail, the amount of methane was measured as a function of pressure. Then, in vacuum condition all the physisorbed molecules were detached from surface of AC and only the chemisorbed molecules could remain connected to it. Therefore, by repeating the methane adsorption for the second time, the quantity of adsorption would show only physisorption of methane. The first and second methane adsorption curves showed completely same quantity of adsorption at each pressure. These results indicate that there is no chemisorption on the surface of prepared ACs. Figure 3a shows the methane adsorption on ACK series as a function of pressures up to 60 Bar at 30 °C. Because the kinetic diameter of methane is bigger than that of N₂ (3.82 and 3.64 Å, respectively), it can be seen that these curves are different with N₂ adsorption results. Less methane adsorption is expected when the adsorbent has low surface area and lacks well-developed pores, as the case of ACK-3. By increasing the activation time and burn-off up to 5 h, there is an increase in methane adsorption. Both ACK-9 and ACK-12 attained same quantity of adsorbed methane at low pressure. This is not the case at high pressure, when ACK-12 shows lower methane adsorption. This is mainly due to widening in micropore size and lack of suitable micropores for methane adsorption. As shown in Fig. 3b, due to different pore size distributions of the ACP series, its adsorbed methane isotherms are highly dispersed when compared to those of the AC and ACK series. The narrow microporosity of ACP-3 and ACP-6 samples resulted in a high degree of adsorption compared to the wider micropores of ACP-9 and ACP-12 samples. The AC series of produced ACs indicate almost the same linear trend of ACK series especially at higher pressures (Fig. 3c). The isotherms of the AC series show higher methane adsorption compared to the ACK series.

Adsorption microcalorimetry of methane on activated carbons samples prepared

The differential enthalpy curve obtained from adsorption microcalorimetric experiments has a global effect that includes both adsorbate–adsorbent as well as adsorbate–adsorbate interactions. Various adsorbate filling mechanisms and phase transitions can be highlighted, as well as any structural changes in the adsorbent. In general, the calorimetric curve highlights various types of behaviors as schematized in Fig. 4. In each system, an increase in the amount of gas adsorbed on a sample leads to an increase in the interactions between the adsorbate molecules. Concerning the adsorbate–adsorbent contributions, the interaction of an adsorbate molecule with an energetically

homogeneous surface will give rise to a constant signal. Finally, in most cases, the adsorbent is energetically heterogeneous due to a pore size distribution and/or a varying surface chemistry (defects, cations, etc.). Initially, one would expect relatively strong interactions between the adsorbing molecules and the surface. The strength of these interactions will then decrease as these specific sites are occupied. Thus, for energetically heterogeneous adsorbents, a gradual decrease in the calorimetric signal is observed. However, each differential enthalpy curve varies and results from the contributions of each interaction.

The differential enthalpies of adsorption-vs-adsorption of CH₄ to the samples prepared in this research from “Cerrejón coal mine (Colombia)” by the three methods used in this research are shown in Fig. 4.

Figure 4a shows the calorimetric isotherms of differential enthalpy of adsorption CH₄ on the four samples of ACK. For the sample ACK-9, the initial decrease in the heat of adsorption (from about 110 to 88 kJ mol⁻¹ at an quantity adsorbed 400 μmol/g), is related to the heterogeneity of the surface as well as also catalytic action between potassium and adsorption of methane. All samples impregnated with KCl at times different exhibit similar behavior in this part, ACK-3, ACK-6, ACK-9 and ACK-12. We can ascribe this region of quantity adsorbed to adsorption on the acid centers of the samples formed during the preparation phase as well as also an interaction between the metal and CH₄. After this region, the curves diverge slightly. For the ACK-9 sample, a plateau is observed that corresponds to filling of the micropore volume still empty. It is energetically homogeneous once the heterogeneous surface adsorption sites are occupied; in this sample, this plateau is presented between 85–80 kJ mol⁻¹ and between 380 and 600 μmol g⁻¹ of sample. In the case of the ACK-12 sample, the plateau presents a small positive slope revealing an increase in the adsorption heat before the final fall. This type of behavior was already quoted in the literature due to the existence of lateral interactions between molecules adsorbed on large cavities in certain porous solids as, for example, zeolites [24, 32–35]. In the present case, however, this hypothesis is not straightforward since the specific adsorption unveiled by the first part of the curve would not favor the occurrence of lateral interactions to interior of structure porous. The sudden drop in the heat of adsorption that follows indicates the completion of micropore filling. For the ACK-6 sample, the curve of the heat of adsorption of CH₄ is distinct: There is neither a clear plateau nor a final decrease in the adsorption heat as seen in the differential enthalpy curves of the ACK-9 or ACK-12. Instead, a smooth decline of the calorimetric isotherm took place between 83 and 79 kJ mol⁻¹, which makes it rather difficult to assign the point where the heat of adsorption changes more significantly in this zone. Tentatively, we have identified the inflection point around

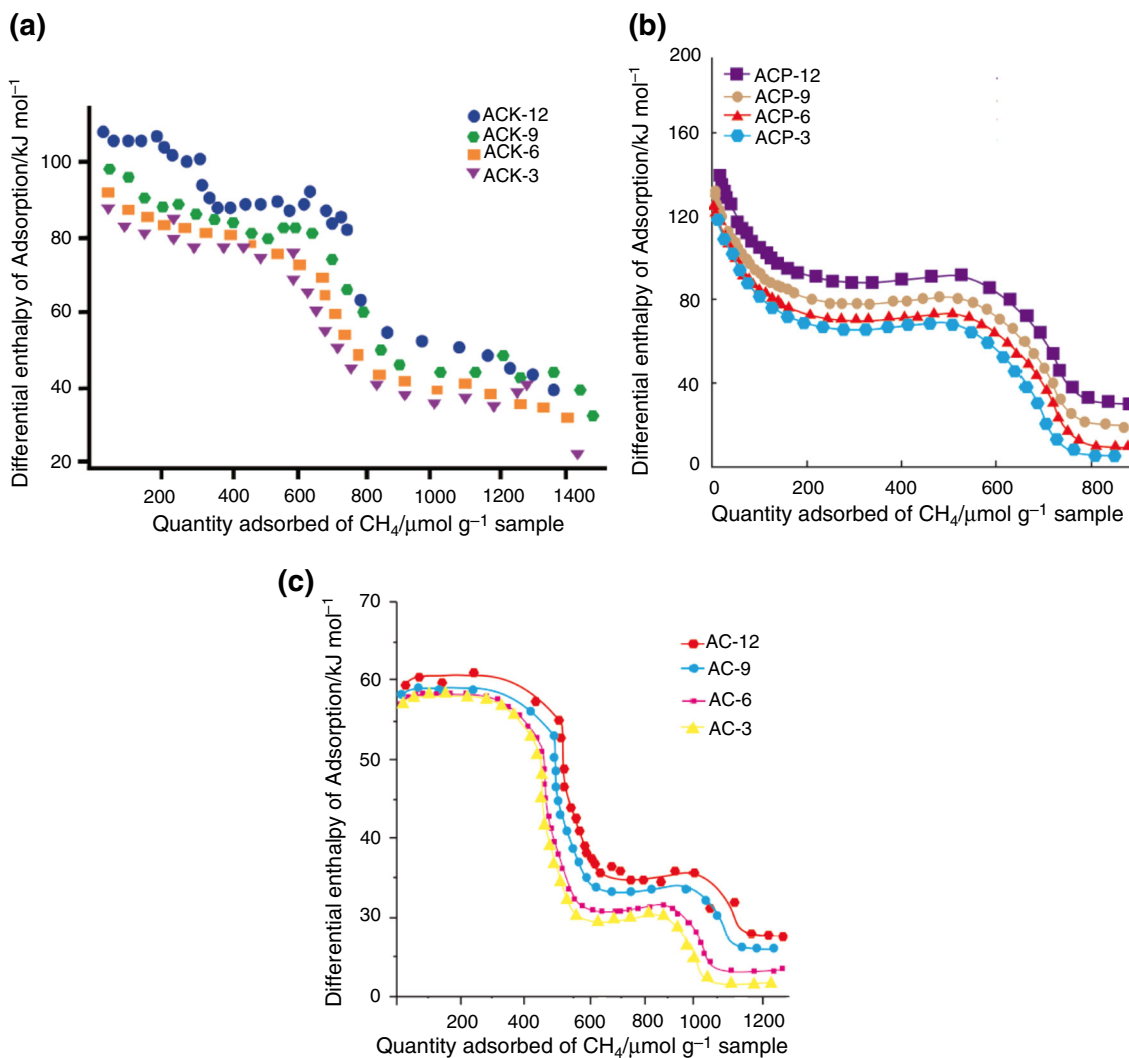


Fig. 4 **a** Differential enthalpies of adsorption of CH₄ on the samples prepared with KCl. **b** Differential enthalpies of adsorption of CH₄ on the samples prepared with H₃PO₄. **c** Differential enthalpies of adsorption of CH₄ on the samples prepared with CO₂

300 μmol g⁻¹, with the conclusion of micropore filling than of the adsorption with CH₄.

The graph corresponding to the ACK-3 sample shows three areas as the previous samples. However, the initial drop in the graph is shorter than in the previous ones which is interpreted as a reduction in the heterogeneity of this sample surface due to the activation time with KCl. The sample ACK-3 not impregnated with any potassium chloride has a different behavior to the above; an initial drop was submitted from 82 kJ mol⁻¹ to about 40 kJ mol⁻¹ which slope slightly later changes to finally reach a final change from 30 kJ mol⁻¹. It is evident that the behavior of the adsorption of CH₄ on the physically activated ACs clearly differ from the results obtained with the samples chemically prepared at high activation times as well as in the differential enthalpies magnitude.

Figure 4b, c shows the results of adsorption enthalpies of samples corresponding to the phosphoric acid and by physical activation method. These charts are different from those obtained with KCl mainly due to potassium's role as a catalyst in the samples prepared by this method. Figure 4b, c has a very similar behavior. Figure 4b shows a slight drop in enthalpy of adsorption at the start of covering with methane which is attributable to a slight heterogeneity formed on the surfaces of the samples resulting from treatment with phosphoric acid and the formation of acid groups. Subsequently all samples reaches a plateau that corresponds to the homogeneously distributed uniform adsorption sites of the samples and then decreases indicating that the monolayer of CH₄ is complete.

In Fig. 4c, differential adsorption enthalpies for samples physically (AC) activated to different activation times are

shown; in these graphs, no drop is observed at the beginning, but it begins to show a plateau for all the samples because of the homogeneity of all samples obtained by this preparation method, which coincides with the analysis in the preceding paragraphs of this research work. Monolayer formed after the enthalpic values fall to the value of the heat of condensation of methane.

Our results show that experimental conditions by adsorption microcalorimetry is possible to follow the process of the adsorption and reaction of CH₄ and its results are in agreement with the results found by adsorption at high pressure. This type of study has not been reported in the literature using this type of activation for analyzing methane storage adsorption microcalorimetry.

Conclusions

In this work, activated carbons obtained from coal from Cerrejon mines (Colombia) were prepared with impregnating with potassium chloride, phosphoric acid and CO₂ to examine their behavior in storage of methane. Samples increased surface area with activation with phosphoric acid and also developed higher micropore volume. The less surface area developed was activated with CO₂.

Methane storage was investigated with isotherms of adsorption at pressure high and adsorption microcalorimetric and its results were compared. The methane storage capacity is very similar to the activated samples using the three methods. This research shows that the activated carbons prepared by coal (from Cerrejon mine (Colombia)), are generally suitable for storage of methane under the conditions of our research. The results obtained by adsorption microcalorimetry are in good agreement as mentioned in the preceding paragraph. It should be noted that the differential enthalpy of adsorption determined for each sample prepared for the adsorption of CH₄ by pulses generated well-defined and different graphs, that allow estimate areas under each curve allowing to evaluate the amount of CH₄ adsorbed on the samples prepared. The highest enthalpic value is presented for samples ACK-9 and ACK-12 obtained by activation with KCl. Additionally adsorption microcalorimetry allows to follow the adsorption process adsorption of CH₄ on activated carbons prepared in this work.

Acknowledgements The authors thank the Universidad de los Andes (Bogotá, Colombia) and Universidad Nacional de Colombia (Sede Bogotá) for the framework agreement between the two institutions under which this research was developed. Special thanks go to the Faculty of Science and the Vice-Rector of Research at the University of the Andes (Bogotá, Colombia) for funding this research.

References

- Zheng Q, Zhu ZW, Wang X. Experimental studies of storage by adsorption of domestically used natural gas on activated carbon. *Appl Therm Eng.* 2015;77:134–41.
- Jordi OS, Xavier G, Joan R. Environmental impacts of natural gas distribution networks within urban neighborhoods. *Appl Energy.* 2009;86:1915–24.
- Wong JW. City-gas development in China-An N.G perspective. *Energy Policy.* 2010;38:2107–9.
- Gao S. The research of adsorption model for methane/hydrogen and thermal effects on storage process. Jimei University of PRC, 2013 (Master's thesis).
- Biloué S, Goetz V, Guillot A. Optimal design of an activated carbon for an adsorbed natural gas storage system. *Carbon.* 2002;40:1295–308.
- Chang KJ, Talu O. Behavior and performance of adsorption natural gas storage cylinders during discharge. *Appl Therm Eng.* 1996;16:359–74.
- Rahman KA, Chakraborty A, Saha BB, Ng KC. On thermodynamics of methane+ carbonaceous materials adsorption. *Heat Mass Transfer.* 2012;55:565–73.
- Rios RB, Bastos-Neto M, Amora MR Jr, Torres EB, Azevedo DCS, Calvacante C Jr. Experimental analysis of the efficiency on charge/discharge cycles in natural gas storage by adsorption. *Fuel.* 2011;90:113–9.
- Policicchio A, MacCallini E, Agostino R, Ciuchi F, Aloise A, Giordano G. Higher methane storage at low pressure and room temperature in new easily scalable large-scale production activated carbon for static and vehicular applications. *Fuel.* 2013;104:813–21.
- Quinn DF, Macdonald JA. Natural gas storage. *Carbon.* 1992;30:1097–103.
- Rahman KA, Loh WS, Chakraborty A, Saha BB, Chun WG, Ng GC. Thermal enhancement of charge and discharge cycles for adsorbed natural gas storage. *Appl Therm Eng.* 2011;31:1630–9.
- Ridha FN, Yunus RM, Rashid M, Ismail AF. Thermal transient behavior of an ANG storage during dynamic discharge phase at room temperature. *Appl Therm Eng.* 2007;37:55–62.
- Sáez A, Toledo M. Thermal effect of the adsorption heat on an adsorbed natural gas storage and transportation. *J Appl Therm Eng.* 2009;39:2617–23.
- Arami-Niya A, Wan Daud WMA, Farouq S. Comparative study of the textural characteristics of oil palm shell activated carbon produced by chemical and physical activation for methane adsorption. *Chem Eng Res Des.* 2011;89:657–64.
- Marsh H, Rodríguez-Reinoso F. *Activated carbon.* Amsterdam: Elsevier; 2006.
- Moreno-Castilla C, Carrasco-Marín F, López-Ramón MV, Alvarez-Merino MA. Chemical and physical activation of olive-mill waste water to produce activated carbons. *Carbon.* 2001;39:1415–20.
- Afrane A. The evolution of the pore structure of coconut shells during the preparation of coconut shell-based activated carbons. *Microporous Mesoporous Mater.* 2008;112:284–90.
- Allwar A, Noor AM, Nawi MABM. Textural characteristics of activated carbons prepared from oil palm shells activated with ZnCl₂ and pyrolysis under nitrogen and carbon dioxide. *J Phys Sci.* 2008;19(2):93–104.
- Gratisito MK, Panyathanmaporn T, Chumnanklang R, Sirinuntawittaya N, Dutta A. Production of activated carbon from coconut shell: optimization using response surface methodology. *Bioresource Technol.* 2008;99:4887–95.
- Nakagawa Y, Molina-Sabio M, Rodríguez-Reinoso F. Modification of the porous structure along the preparation of activated carbon monoliths with H₃PO₄ and ZnCl₂. *Microporous Mesoporous Mater.* 2007;103:29–34.

21. Prauchner M, Rodríguez-Reinoso F. Preparation of granular activated carbons for adsorption of natural gas. *Microporous Mesoporous Mater.* 2008;109:581–4.
22. Rouquerol J, Rouquerol F, Sing KS. *Adsorption by powders and porous solids: principles, methodology and applications.* London: Academic Press; 1999.
23. Şentorun-Shalaby Ç, Uçak-Astarlıoğlu MG, Artok L, Sarici Ç. Preparation and characterization of activated carbons by one-step steam pyrolysis/activation from apricot stones. *Microporous Mesoporous Mater.* 2006;88:126–34.
24. Mozammel H, Masahiro O, Bhattacharya SC. Activated charcoal from coconut shell using $ZnCl_2$ activation. *Biomass Bioenergy.* 2002;22:397–400.
25. Molina-Sabio M, Almansa C, Rodríguez-Reinoso F. Phosphoric acid activated carbon discs for methane adsorption. *Carbon.* 2003;41:2113–9.
26. Pillai R, Sunil P, Raksh J. Adsorption of carbon dioxide, methane, nitrogen, oxygen and argon in NaETS-4. *Microporous Mesoporous Mater.* 2008;113:268–76.
27. Hu Z, Guo H, Srinivasan MP, Yaming NA. Simple method for developing mesoporosity in activated carbon. *Sep Purif Technol.* 2003;31:47–52.
28. Ismadji S, Bhatia SK. A modified pore filling isotherm for liquid phase adsorption in activated carbon. *Langmuir.* 2003;17:1488–98.
29. Devarly PY, Kartika N, Indraswati S. Activated carbon from jack-fruit peel waste by H_3PO_4 chemical activation: pore structure and surface chemistry characterization. *Chem Eng J.* 2008;140:32–42.
30. Suzuki RM, Andrade AD, Sousa JC, Rollemberg MC. Preparation and characterization of activated carbon from rice bran. *Bioresource Technol.* 2007;98:1985–91.
31. Thommes M, Kaneko K, Neimark AV, Olivier JP, Rodríguez-Reinoso F, Rouquerol J, Sing KSW. *Physisorption of gases, with special reference to the evaluation of surface area and pore size distribution (IUPAC Technical Report).* *Pure Appl Chem.* 2015;87(9–10):1051–69.
32. Yang T, Chong LA. Textural and chemical properties of zinc chloride activated carbons prepared from pistachio-nut shells. *Mater Chem Phys.* 2006;100:438–44.
33. Moreno-Piraján JC, García-Cuello VS, Giraldo L. Characterization of mordenite-supported Pd, Pt, and Ir determined by CO adsorption microcalorimetry and the dehydrogenation reaction of C3 alkanes. *Top Catal.* 2011;54:146–52.
34. Llewellyn P, Maurin G. Gas adsorption microcalorimetry and modelling to characterise zeolites and related materials. *Chimie.* 2005;8:283–302.
35. Spirewak BE, Dumesic JA. Applications of adsorption microcalorimetry for the characterization of metal-based catalyts. *Themochimica acta.* 1998;312:95–104.